Time-resolved fluorescence spectroscopy for the diagnosis of oral lichen planus

Gorpas D.[†], Davari P., Bec J., Fung M.A., Marcu L., Farwell G., Fazel N.

This study was conducted between 01/24/2014 and 04/10/2015 at the University of California, Davis Medical Center, Sacramento, California, United States of America.

Corresponding Author: **Fazel Nasim**, Department of Dermatology, University of California, Davis, 3301 C Street, Sacramento, CA 95816. tel: (916) 734-6876, nfazel@ucdavis.edu

Keywords: oral lichen planus, fluorescence lifetime, time-resolved fluorescence spectroscopy, fluorescence lifetime guided diagnosis.

Manuscript word count: 1871 (excl. title page, abstract, and references)

Figure count: 4

Conflict of interest disclosures: All authors declare no conflict of interest.

Short Title: Fluorescence lifetime of oral lichen planus

[†]**Current address**: Institute of Biological and Medical Imaging, Helmholtz Zentrum München, Germany.

Bulleted statements

what's already known about this topic?

- Oral lichen planus (OLP) is considered a potentially malignant disorder with increased risk of oral squamous cell carcinoma.

- OLP diagnosis is based on clinicopathological correlation, which has showed to be only mild to moderate.

- There is an unmet need for novel diagnostic methods with better accuracy and reproducibility.

what does this study add?

- Time-resolved fluorescence spectroscopy (TRFS) has the potential to differentiate OLP from peri-lesional normal tissue.

- Multispectral-TRFS (ms-TRFS) can provide non-invasive real-time OLP diagnosis with minimal risk to the patient.

ABSTRACT

Background. Lichen planus is a T-cell mediated autoimmune disorder of unknown etiology that affects the skin, nails, oral and genital mucous membranes. Conventionally, oral lichen planus (OLP) is diagnosed through clinical assessment and histopathologic confirmation by oral biopsy.

Aim. In this pilot study, we explore the use of time-resolved fluorescence spectroscopy (TRFS) to detect fluorescence lifetime changes between lesional OLP and peri-lesional normal mucosa.

Methods. Measurements of lesional and peri-lesional buccal and floor of mouth mucosa were conducted *in vivo* with a TRFS system. Histopathologic confirmation was consistent with OLP in 8 out of 10 patients biopsied. Two patients with histopathological diagnoses of frictional hyperkeratosis and oral candidiasis, respectively, were excluded from the study.

Results. Our preliminary data show that lifetime values in the 360-560 nm spectral range, indicate a significant differentiation between normal and diseased tissue. In contrast to the standard oral biopsy procedure, this technique is non-invasive, painless, time-efficient, and safe.

Conclusions. Future studies are needed to better elucidate its diagnostic capability and to further explore the sources of fluorescence contrast. This pilot study suggests that based on fluorescence lifetime parameters, TRFS is a very promising technology for the development of a novel OLP diagnostic technique.

Introduction

Lichen planus is a T-cell mediated autoimmune disorder of unknown etiology with an estimated prevalence of 0.22% to 5% worldwide (1). It is a chronic mucocutaneous disorder that affects the skin, nails, hair, and mucous membranes including the oral, vulvovaginal, laryngeal, esophageal, and conjunctival mucosa (2, 3). It is considered a potentially malignant disorder with increased risk of oral squamous cell carcinoma (4, 5).

The diagnosis of oral lichen planus (OLP) is based on clinicopathological correlation. However, a lack of validated clinical or histologic criteria, and substantial inter-observer variability has been documented for both clinical and histologic assessment (6-8). A recent study showed only mild to moderate clinicopathological correlation in the diagnosis of OLP (9). The absence of histopathologic correlation may reflect variation in the nature (i.e. erosive vs. hyperkeratotic), chronicity and location of OLP lesions. Thus, more reliable methods for diagnostic confirmation can be invaluable in the timely diagnosis and treatment of OLP given its premalignant nature and associated morbidity.

The relative accessibility of the oral cavity lead to the development of many spectroscopic and imaging devices to assess various lesion types. Most of the studies in head and neck cancer are based on either steady-state spectroscopy or intensity imaging. These techniques lack specificity due to intra- and inter- patient variability and the relatively large number of factors that influence their functionality (10). In order to improve specificity most of these studies included complementary diagnostic techniques, such as diffuse reflectance spectroscopy (11, 12), light scattering spectroscopy (11), depth sensitive probes (12), and digital image processing (13). Fluorescence lifetime techniques have demonstrated that fluorescence decay dynamics can effectively discriminate oral squamous carcinoma tumors from normal tissue (14-16).

In this pilot study, we investigate whether fluorescence lifetime can provide a means of differentiation between OLP and peri-lesional normal mucosa. Specifically, we performed *in vivo* time-resolved fluorescence spectroscopy (TRFS) measurements on oral mucosa using two complementary approaches, as described in the study.

Methods

Patients

This study was approved by the Institutional Review Board at the University of California, Davis and was carried out in accordance with the Declaration of Helsinki protocols. Ten patients were enrolled and all measurements were obtained prior to punch biopsy procedure. TRFS measurements were obtained *in vivo* from clinically normal appearing peri-lesional mucosa and OLP lesional mucosa. The clinical assessment was blind to TRFS measurements. Five points were measured (i.e. center, superior, inferior, anterior, and posterior poles) from each anatomical site. Following these measurements linear scans were acquired from the OLP suspected areas for 8 of the 10 patients, to record the transition from the peri-lesional normal tissue to the lesions. All scans were registered to the five points to optimize comparison with histopathological analysis. Lesional tissue was fixed in 10% neutral buffered formalin and submitted for routine processing. Peri-lesional normal tissue was placed in Michel's transport media and routinely processed for direct immunofluorescence testing. All samples were handled, tested, and interpreted by a board certified dermatopathologist (MAF) blind to TRFS measurements.

Time-Resolved Fluorescence Spectroscopy

Tissue autofluorescence was induced by a 337 nm pulsed nitrogen laser (MNL 205, LTB Lasertechnik). Excitation light was delivered to the interrogated locations through a 3 m long

0.48 NA polymer clad multimode fibre (BFH48-400, Thorlabs, Inc.). The emitted fluorescence was collected by the same fibre and guided to an optical apparatus consisting of a moving mirror (element M in Fig. 1). The location of the mirror defined whether the collected fluorescence was spectrally resolved sequentially over the entire spectrum or simultaneously over three predefined spectral bands. For the first mode of operation the emitted fluorescence was spectrally resolved (360-600 nm range, 10 nm interval) by an imaging spectrometer/monochromator (MicroHR, f/3.8, 600 g/mm grating; Horiba Jobin Yvon), detected with a gated multichannel plate photomultiplier tube (MCP-PMT, R3809U-50, Hamamatsu, 45ps FWHM) and temporally resolved by a fast digitizer at 125 ps time intervals (U1065A-DC252, Agilent Acqiris).

During the second mode of operation, the emitted fluorescence was guided into a wavelength selection module (WSM) composed of dichroic and band-pass filters that simultaneously spectrally resolve the collected signal in three channels: 390/40 nm (channel 1), 466/40 nm (channel 2), 542/50 nm (channel 3) (17). The three signals were then detected by a single non-gated multichannel plate photomultiplier (MCP-PMT, R3809U-50, Hamamatsu, 45 ps FWHM) and temporally resolved by the same fast digitizer described above.

The system was placed in a cart suitable for use in the examination room. A foot pedal provided the control of the data acquisition, while the switch between systems was implemented through software control. The excitation/collection fibre, Fig. 1, was long and flexible enough to permit measurements within the oral cavity. Use of the device doesn't require any specialized or advanced training.

The data analysis and system control were implemented with MATLAB (Mathworks, Inc) and LabVIEW (National Instruments) respectively (18, 19). Measurements from the two tissue groups were tested using univariate statistical analysis (one-way ANOVA) to identify whether lifetime measurements could differentiate the two tissue types.

Results and Discussion

Seven out of 10 biopsies taken from suspected OLP lesions confirmed a clinical diagnosis of OLP. One biopsy showed sparse, non-specific changes, which could not support or exclude OLP. However, clinical examination of this case was consistent with classic reticulated and erosive OLP and as such categorized as OLP positive. The 2 cases excluded were diagnosed as frictional hyperkeratosis and oral candidiasis, respectively. The mucosal location of the biopsy sites included 2 samples taken from the right buccal mucosa (OLP positive), 6 samples from the left buccal mucosa (4 OLP positive, 1 diagnosed as frictional keratosis and 1 as oral candidiasis), 1 sample from the left floor of mouth (OLP positive), and 1 from the left mandibular sulcus (OLP positive). TRFS measurements acquired from patients diagnosed with OLP were considered in this study, leading to a total of 8 OLP-normal mucosa sample pairs.

Autofluorescence intensity revealed significant differentiation between normal mucosa and OLP lesions at the 370 to 420 nm spectral band, which is primarily attributed to collagen and secondarily to elastin (20). The normalized integrated intensity values (each spectrum was normalized to unit value) revealed a shift towards higher wavelengths for OLP as compared to peri-lesional normal mucosa (Fig. 2a). This differentiation can be attributed to the presence of less collagen and elastin fibres in the OLP lesional tissue. This is better illustrated in the histologic images shown in Figs 2d and 2e. The ~300 μm penetration depth of excitation light in OLP lesional tissue (Fig. 2d) is largely or exclusively limited to the epithelium whereas in peri-lesional normal tissue (Fig. 2e) this depth extends into the lamina propria. The rich collagen and elastin component of the lamina propria leads to higher fluorescence signals (Fig. 2b).

In addition, the intensity from both OLP and normal tissues at the 420 nm to 480 nm band can be attributed to the presence of nicotinamide adenine dinucleotide (NADH) (20). As shown in Fig.

2a, OLP and normal tissue present minor differentiation at this spectral band, in contrast to oral squamous cell carcinoma where this difference is much stronger and statistically significant (15). The increased cell and metabolic activity of squamous cell carcinoma associated with the progression of neoplastic disease, leads to increased NADH binding to proteins resulting in increased fluorescence emission at the 420 nm to 480 nm spectral band (11, 21). On the other hand, the lack of this signal for the OLP cases could potentially be attributed to the absence of this cell and metabolic activity. Nevertheless, such assumption requires further and systematic investigation.

Fluorescence intensity measurements are influenced by various experimental conditions, including intra- and inter- patient variability, changes in excitation-collection coupling due to tissue motion and/or surface geometry, the presence of intrinsic absorbers, and the photobleaching effect (22). Considering all measurements were taken in a non-contact mode, the experimental conditions may explain the relatively high standard deviation values of measured intensity over the entire spectrum (Figs 2a and 2b). This is further supported by Fig. 2f, which depicts a clinical image of a representative case. The increased inhomogeneity of the lesional area influences (1) the excitation-collection coupling and (2) the intensity of the emitted signal due to intrinsic absorption and/or scattering, that is different locations on the same lesion may lead to different fluorescence intensity readouts.

Fluorescence lifetime, on the other hand, is independent of all these experimental conditions (23-25). Fig. 2c illustrates the lifetime spectra from the normal and OLP tissues, as derived from the time-resolved fluorescence measurements. Fluorescence lifetime spectra differentiate between the normal and diseased tissues over the entire measured spectrum, and for normal tissue are consistent with our previous studies (15). Another important observation is that the lifetime values of OLP tissues appear to be lower than that of cancerous tissue (15).

These results are further validated by the ms-TRFS measurements, Fig. 3a. Specifically, the derived lifetime values at the three ms-TRFS channels (390/40 nm, 466/40 nm, and 560/46 nm) were 1.5±0.3 ns, 1.2±0.3 ns, and 1.1±0.3 ns for normal tissue and 0.8±0.2 ns, 0.8±0.2 ns, and 0.9±0.3 ns for OLP tissues, respectively. These values are consistent with the corresponding values from the TRFS measurements as shown in Fig. 2c (i.e. 1.4±0.5 ns, 1.3±0.5 ns, and 1.3±0.5 ns versus 0.8±0.3 ns, 0.7±0.2 ns, and 0.7±0.2 ns, respectively). This consistency of the derived lifetime values from the two systems highlights the robustness of lifetime measurements, when compared to intensity measurements.

Although this study is limited by a small patient population, statistical analysis via one-way ANOVA test indicates statistically significant differentiation between normal and OLP tissue lifetime measurements ($p < 0.001$). These results are depicted in Fig. 4 for data at two spectral bands acquired by both systems employed in this study.

A weakness of this study is the limited number of specimens analyzed. Thus, the promising results concluded from this study support the need for further large scale studies to develop a diagnostic algorithm for OLP. In addition, the two cases not included in the study showed differentiation in both intensity and lifetime spectra (data not shown), however, further examination of specimens would be required to confirm this observation. Thus, the significant clinical need remaining to be addressed is quantification of the discrimination power of lifetime measurements to distinguish OLP from other oral mucosal conditions with similar clinical morphology.

Conclusion

The current gold standard for the diagnosis of OLP is clinicohistopathological correlation. However, studies have shown significant limitations to reliably establishing a diagnosis by this

method including insufficient reproducibility, intraobserver and interobserver variability and mild to moderate clinicopathological correlation. Thus, there is an unmet need for novel diagnostic methods with better accuracy and reproducibility. Time-resolved fluorescence spectroscopy, as a potential non-invasive, real-time diagnostic method, also has the advantage of being painless with minimal risk and is more time efficient. The results of our study show promise for the use of TRFS as a potential diagnostic tool that could be utilized as an adjunct to clinical examination, reduce the number of unnecessary biopsies by highlighting specific regions of interest, and serve as an alternative to punch biopsy for patients refusing the procedure. Moreover, our observations suggest the need for larger scale studies to further investigate its potential application for OLP diagnosis.

References

1. Gorouhi F, Davari P, Fazel N. Cutaneous and Mucosal Lichen Planus: A Comprehensive Review of Clinical Subtypes, Risk Factors, Diagnosis, and Prognosis. Scientific World J. 2014;2014:742826 1-22.

2. Gupta S, Jawanda M. Oral lichen planus: An update on etiology, pathogenesis, clinical presentation, diagnosis and management. Indian J Dermatol. 2015;60(3):222-9.

3. Silverman SJ, Bahl S. Oral lichen planus update: clinical characteristics, treatment responses, and malignant transformation. Am J Dent. 1997;10(6):259-63.

4. Abbate G, Foscolo AM, Gallotti M, et al. Neoplastic transformation of oral lichen: case report and review of the literature. Acta Otorhinolaryngol Ital. 2006;26(1):47-52.

5. Bombeccari GP, Guzzi G, Tettamanti M, et al. Oral lichen planus and malignant transformation: a longitudinal cohort study. Oral Surg Oral Med Oral Pathol Oral Radiol Endod. 2011;112(3):328-34.

6.   Van Der Meij EH, Van Der Waal I. Lack of clinicopathologic correlation in the diagnosis of oral lichen planus based on the presently available diagnostic criteria and suggestions for modifications. J Oral Pathol Med. 2003;32(9):507-12.

7.   van der Meij EH, Reibel J, Slootweg PJ, et al. Interobserver and intraobserver variability in the histologic assessment of oral lichen planus. J Oral Pathol Med. 1999;28(6):274-7.

8.   Van Der Meij EH, Schepman KP, Plonait DR, et al. Interobserver and intraobserver variability in the clinical assessment of oral lichen planus. J Oral Pathol Med. 2002;31(2):95-8.

9.   Hiremath S, Kale AD, Hallikerimath S. Clinico-pathological study to evaluate oral lichen planus for the establishment of clinical and histopathological diagnostic criteria. Turk Patoloji Derg. 2015;31(1):24-9.

10.   Gorpas D, Marcu L. Fluorescence Lifetime Spectroscopy and Imaging Techniques in Medical Applications. In: Olivo M, Dinish SU, editors. Frontiers in Biophotonics for Translational Medicine: In the Celebration of Year of Light (2015). Singapore: Springer Singapore; 2016. p. 1-46.

11.   Muller MG, Valdez TA, Georgakoudi I, et al. Spectroscopic detection and evaluation of morphologic and biochemical changes in early human oral carcinoma. Cancer. 2003;97(7):1681-92.

12.   Schwarz RA, Gao W, Redden Weber C, et al. Noninvasive evaluation of oral lesions using depth-sensitive optical spectroscopy. Cancer. 2009;115(8):1669-79.

13.   Roblyer D, Kurachi C, Stepanek V, et al. Objective detection and delineation of oral neoplasia using autofluorescence imaging. Cancer Prev Res. 2009;2(5):423-31.

14.   Chen H-M, Chiang C-P, You C, et al. Time-resolved autofluorescence spectroscopy for classifying normal and premalignant oral tissues. Laser Surg Med. 2005;37(1):37-45.

15. Meier JD, Xie H, Sun Y, et al. Time-resolved laser-induced fluorescence spectroscopy as a diagnostic instrument in head and neck carcinoma. Otolaryngol Head Neck Surg. 2010;142(6):838-44.

16. Sun Y, Phipps JE, Meier J, et al. Endoscopic fluorescence lifetime imaging for in vivo intraoperative diagnosis of oral carcinoma. Microsc microanal. 2013;19(4):791-8.

17. Yankelevich DR, Ma D, Liu J, et al. Design and evaluation of a device for fast multispectral time-resolved fluorescence spectroscopy and imaging. Rev Sci Instrum. 2014;85(3):034303.

18. Ma D, Bec J, Gorpas D, et al. Technique for real-time tissue characterization based on scanning multispectral fluorescence lifetime spectroscopy (ms-TRFS). Biomed Opt Express. 2015;6(3):987-1002.

19. Liu J, Elson DS, Marcu L. Analysis of time-domain fluorescence measurements using least-squares deconvolution. Fluorescence Lifetime Spectroscopy and Imaging: CRC Press; 2014. p. 249-68.

20. Wagnieres GA, Star WM, Wilson BC. In vivo fluorescence spectroscopy and imaging for oncological applications. Photochem Photobiol. 1998;68(5):603-32.

21. Fatakdawala H, Poti S, Zhou F, et al. Multimodal in vivo imaging of oral cancer using fluorescence lifetime, photoacoustic and ultrasound techniques. Biomed Opt Express. 2013;4(9):1724-41.

22. Lakowicz JR. Principles of Fluorescence Spectroscopy. 3rd ed. New York: Springer; 2006. 954 p.

23. Becker W. Fluorescence lifetime imaging-techniques and applications. J Microsc. 2012;247(2):119-36.

24.   Cubeddu R, Comelli D, D'Andrea C, et al. Time-resolved fluorescence imaging in biology and medicine. J Phys D-Appl Phys. 2002;35(9):R61-R76.

25.   Marcu L, Jo JA, Butte P. Fluorescence Lifetime Spectroscopy in Cardio and Neuroimaging. In: Iftimia N., Brugge WR, Hammer DX, editors. Advances in Optical Imaging for Clinical Medicine. New Jersey: Wiley; 2011. p. 255-85.

Figures
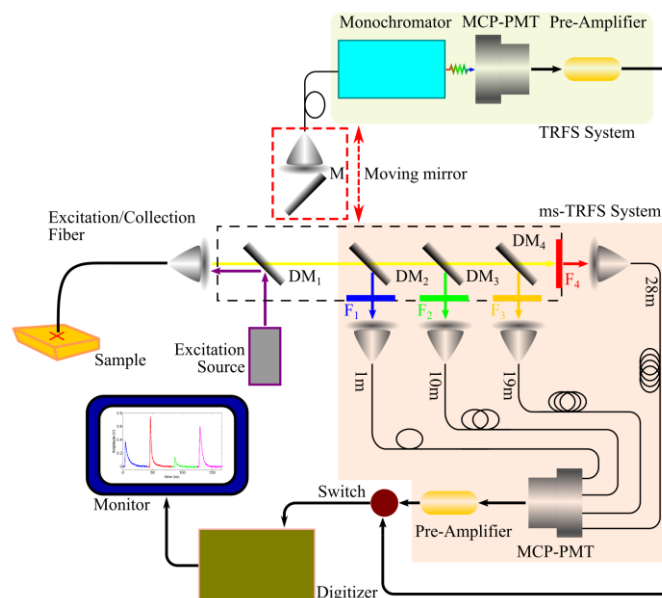
Figure 1: A schematic of the employed system, depicting the TRFS and ms-TRFS modules. F_1: 390/40 nm; F_2: 466/40 nm; F_3: 542/50; F_4: 629/53 nm (not used in current study); DM_1: 370 nm dichroic mirror; DM_2: 425 nm; DM_3:515 nm; DM_4: 610 nm; M: Moving mirror that controls the operating module (i.e if positioned between DM1 and DM2 then TRFS measurements are implemented, else ms-TRFS measurements are acquired).
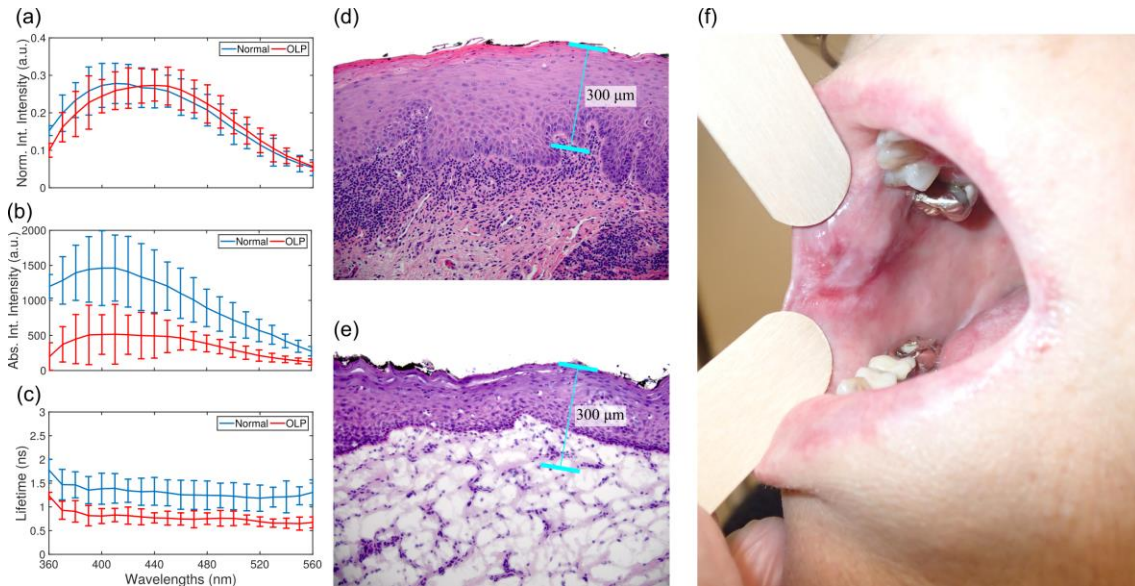
Figure 2: Time-resolved fluorescence spectroscopy measurements from the 8 patients considered in this study. (a) The normalized and (b) absolute values of the integrated autofluorescence intensity, and (c) the corresponding lifetime values. (d) Section from an OLP punch biopsy sample stained with H&E. (e) Section from a normal peri-lesional tissue punch biopsy sample stained with fluorescein-conjugated antibodies (albumin, IgA, IgM, IgG, C3, fibrinogen). The difference in the spectra between diseased and normal tissues at the spectral region 370 nm to 420 nm can be attributed to the relative absence of subepithelial collagen and elastin in OLP (d) compared to normal peri-lesional tissue (e) as captured by the typical 300 μm penetration depth of the 337 nm excitation light. (f) Hyperkeratotic patch with focal erosions involving the right buccal mucosa. The errorbars correspond to mean+/-SD.
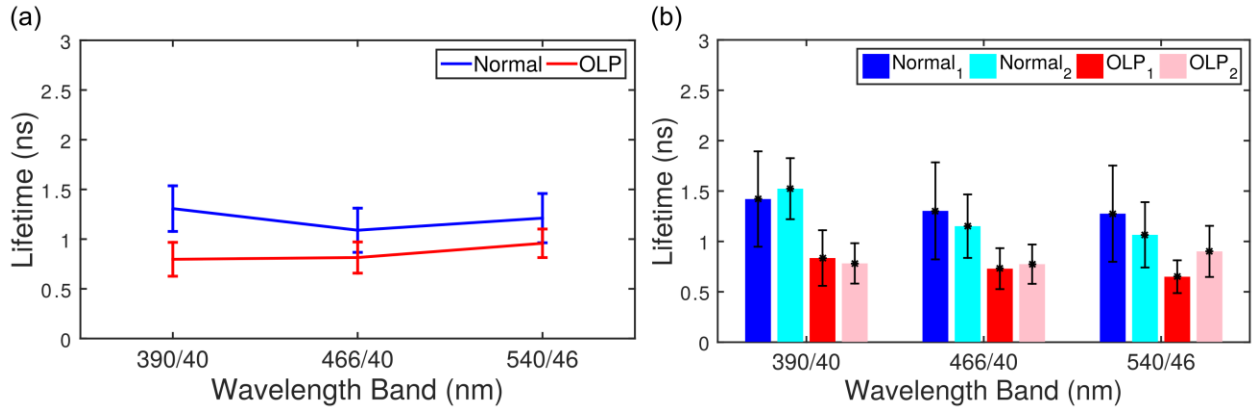
Figure 3: Multi-spectral fluorescence lifetime measurements. (a) The derived lifetime values at three specific spectral bands. (b) Lifetime values as estimated by the data acquired from both systems at three spectral bands and for both normal and OLP tissues. The errorbars correspond to mean+/-SD.
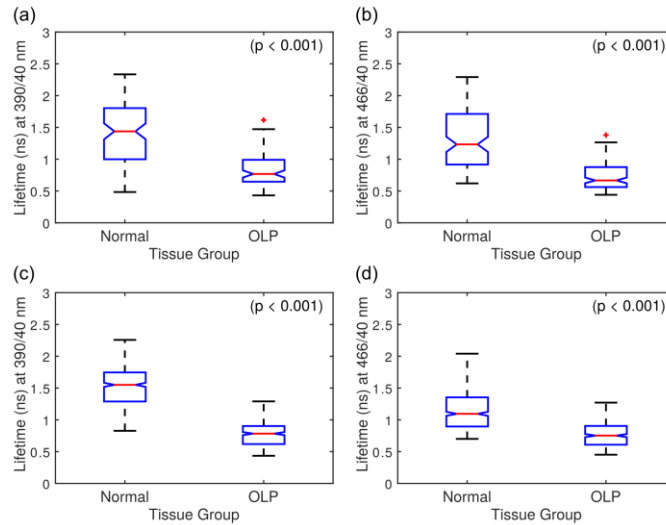
Figure 4: Lifetime differentiation between peri-lesional normal mucosa and OLP lesional tissues. (a) Differentiation at the 390/40 nm and (b) at the 466/40 nm spectral bands as derived from data acquired by the TRFS system. (c) and (d) The corresponding differentiation as derived from data acquired by the ms-TRFS system.